EFFECT OF OLEFINS ON HYDRODESULFURIZATION OF A CRACKED NAPHTHA REFORMER FEED

By

DONALD PRENTICE SATCHELL, JR.

Bachelor of Science

Michigan State University

East Lansing, Michigan

1969

Submitted to the Faculty of the Graduate College
of the Oklahoma State University
in partial fulfillment of the requirements
for the Degree of
MASTER OF SCIENCE
July, 1972

EFFECT OF OLEFINS ON HYDRODESULFURIZATION OF A CRACKED NAPHTHA REFORMER FEED

Thesis Approved:

B. L. Crynes
Thesis Adviser

Robert L. Robinson, Jr.

D. Durham
Dean of the Graduate College

PREFACE

In the past, a very empirical approach has been taken to the analysis of hydrodesulfurization of petroleum fractions. This work is a mechanistic analysis of the effect of olefin content on the rate of hydrodesulfurization of a naphtha. Hopefully, it will serve as a small step toward a more mechanistic understanding of hydrodesulfurization of petroleum stocks in general.

I would like to thank my major adviser, Dr. B. L. Crynes, for his encouragement during the course of the study. I am indebted to the School of Chemical Engineering for support during the period of the project.

TABLE OF CONTENTS

LIST OF TABLES

LIST OF FIGURES

NOMENCLATURE

A, b, and c	arbitrary constants
(a)	adsorbed specie
Br	bromine number
C_i	concentration of adsorbed specie i
$D_{i,m}$	diffusivity of component i
dp	diameter of catalyst particle
G	reactant mass flux based on total reactor cross section
(g)	specie in vicinity of catalyst surface
k_i	constant introduced in Equation i
N_{RE}	Reynolds number, dpG/μ
N_{SC}	Schmidt number, $\mu/\rho D$
P_i	partial pressure of specie i
S	sulfur concentration, ppm
s	slope of a plot of the common logarithm of bromine number as a function of space time
X	fraction of organosulfur species desulfurized
y_i	mole fraction of component i
z	catalyst bed height
Θ	space time - catalyst bed volume/oil volumetric flow rate

μ	reactant viscosity at reactor operating conditions
ρ	reactant density at reactor operating conditions

Subscripts

E	unoccupied active site
HC	average over the high conversion region
H_2S	hydrogen sulfide
O	olefin
T	thiol
TS	total sulfur
iRX	i reactors in series

Superscripts

f	evaluated at the reactor outlet
o	evaluated at the reactor inlet
Θ	evaluated at space time Θ
+	forward reaction
-	reverse reaction

Abbreviations

HDS	hydrodesulfurization
ppm	parts per million
psig	pounds per square inch guage
R	hydrocarbon
Rx	reactor
S	sulfur
SCF	standard cubic feet
SCFH	standard cubic feet per hour
°F	degree Fahrenheit

CHAPTER I

INTRODUCTION

Refinery experience has shown that a cracked naphtha is more difficult to hydrodesulfurize than a virgin naphtha. A naphtha is a petroleum fraction with the approximate initial true boiling point of 80°F and an end point of 400°F. A cracked naphtha is a product, in the naphtha boiling range, of a process that results in the rupture of a significant fraction of the carbon-carbon bonds in the feed to that process. A virgin naphtha is a petroleum fraction, in the naphtha boiling range, that has been subjected to distillation only. This work will develop a kinetic model for hydrodesulfurization of a cracked naphtha to rationalize the additional difficulties encountered when hydrodesulfurizing a cracked rather than a virgin naphtha.

Desulfurization Technology

Definition of Hydrodesulfurization

Hydrodesulfurization will be defined as the hydrogenolysis of organosulfur species to H_2S and the corresponding paraffin. Reactions 1, 2, and 3 illustrate hydrodesulfurization of the major classes of organosulfur species found in petroleum stocks.

$$\underset{\text{(R-S-H)}}{\text{Thiol}} + H_2 \longrightarrow H_2S + \underset{\text{(R-H)}}{\text{Paraffin}} \qquad (1)$$

$$\underset{(R\text{-}S\text{-}R^1)}{\text{Sulfide}} + 2H_2 \longrightarrow H_2S + 2\ \underset{(R\text{-}H,\ R^1\text{-}H)}{\text{Paraffin}} \qquad (2)$$

$$\underset{\substack{R\text{-}R^1 \\ S}}{\text{Ring Sulfur}} + 2H_2 \longrightarrow H_2S + \underset{(H\text{-}R\text{-}R^1\text{-}H)}{\text{Paraffin}} \qquad (3)$$

Typical Reactor Operating Conditions

Hydrodesulfurization of a naphtha is typically carried out in the temperature range of 500°F to 800°F, with pressures of 300 to 600 psig, and hydrogen flows from 300 to 1500 standard cubic feet per petroleum barrel. Total sulfur concentrations in the feed usually lie in the range of 100 to 1000 ppm (parts per million of elemental sulfur on a weight basis). Economic reformer operation requires a desulfurizer effluent with less than 2 ppm total sulfur (1). Thus, the hydrosulfurization (HDS) reactor must reduce the naphtha to at least this sulfur level.

Figure 1 is a diagram of a typical system to hydrodesulfurize a reformer feed. If hydrogen is recycled to the HDS reactor through a high pressure separator (as shown in Figure 1), then the hydrogen produced in the reformer is usually sufficient to meet the hydrogen demand of the HDS reactor. Typically, about half of the H_2S in the reactor effluent is recycled with the hydrogen when a high pressure separator is used. This recycled H_2S will later be shown to have a marked effect on the reactor performance.

In the past, rate expressions of the following general form (Equation 4) have been used to describe the kinetics of gas phase hydrodesulfurization of petroleum fractions.

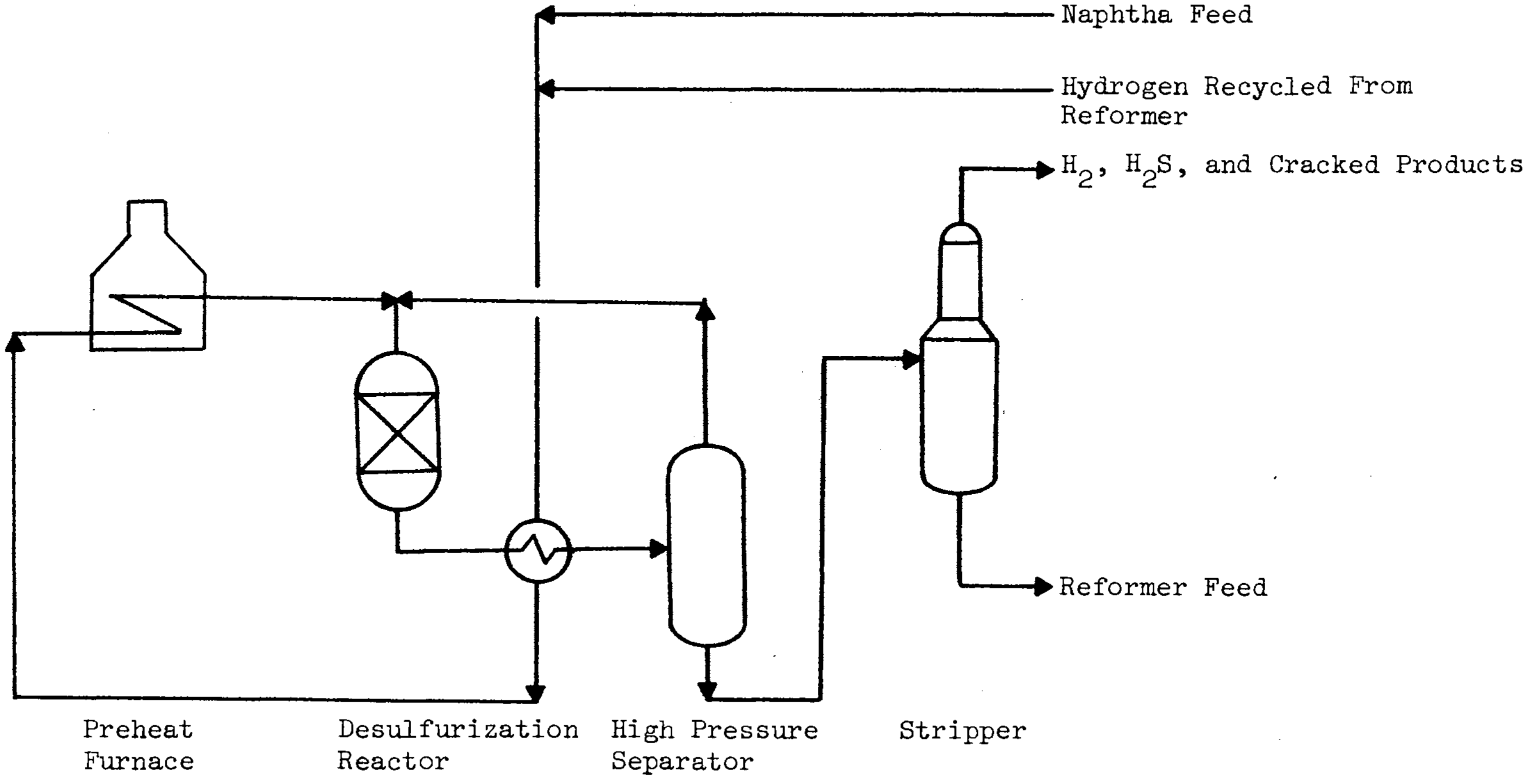

Figure 1. Flow Diagram of a Typical Hydrodesulfurization Unit to Pretreat a Reformer Feed

$$\text{Rate of Organosulfur Removal} = A\, P_{TS}^{b}\, P_{H_2}^{c} \tag{4}$$

P_{TS} and P_{H_2} are the partial pressures of organosulfur species and hydrogen respectively. A, b, and c are arbitrary constants. This rate expression implicitly assumes that hydrogenolysis is the only significant reaction of organosulfur species in a commercial HDS reactor. Some pure component studies (2, 3) indicate that other reactions may be important. Although this empirical approach has been reasonably successful in describing the kinetics of virgin naphtha desulfurization, difficulties arise when it is applied to severe hydrodesulfurization of a cracked naphtha.

Figure 2 is a plot of the logarithm of total organosulfur concentration (ppm) as a function of space time (catalyst volume/oil volumetric flow for a cracked naphtha feed.) The data are given in Appendix A. Such a plot might be expected to form a straight line if desulfurization were first order with respect to total sulfur concentration. However, the data presented in Figure 2 appear to form two distinct lines. This type of kinetic behavior is difficult to rationalize with the empirical rate expression, Equation 4.

There are at least three possible approaches to rationalizing the data presented in Figure 2 in terms of Equation 4.

1. The sudden reduction in the rate of desulfurization could be the result of approaching a thermodynamic limit. However, a study (4), using ideal state free energies, showed that there is probably no thermodynamic limitation to hydrodesulfurization

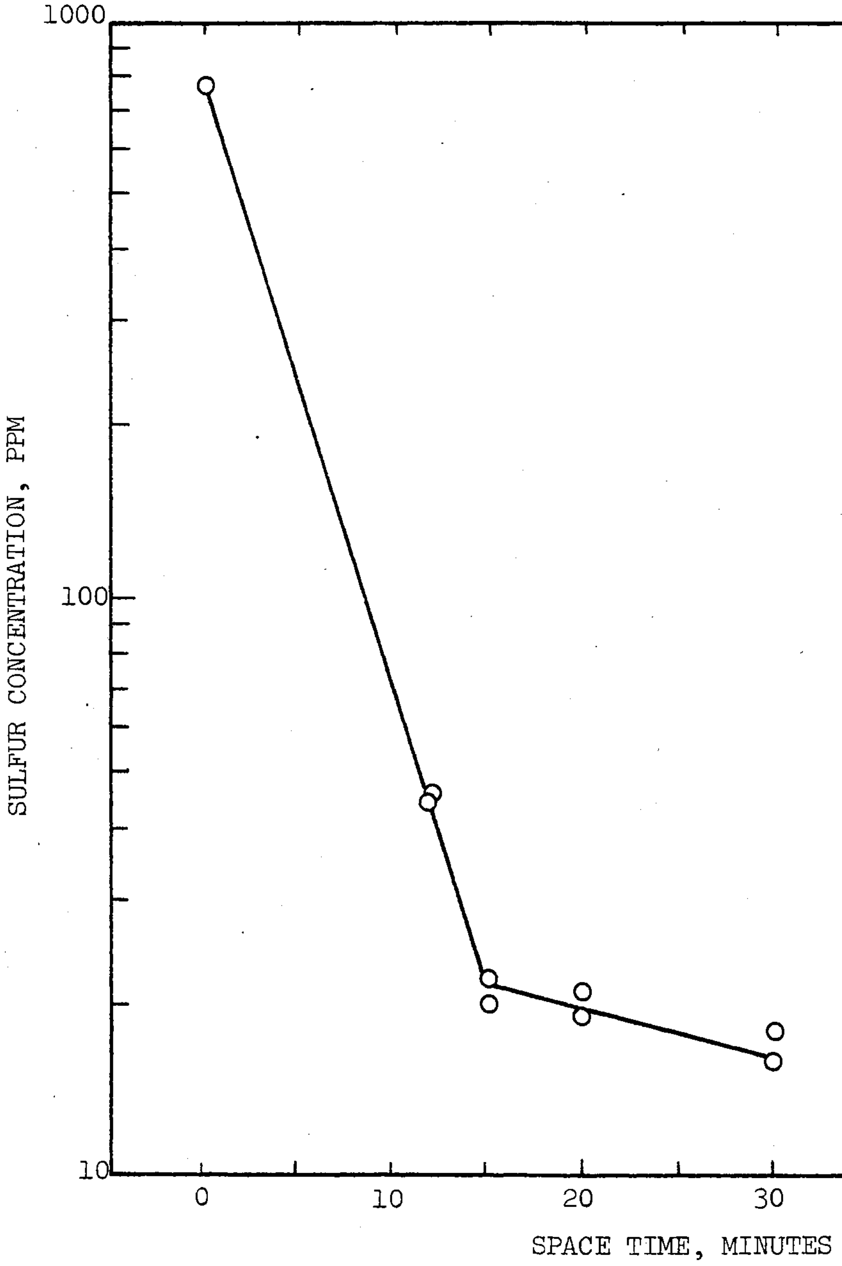

Figure 2. Total Sulfur Concentration as a Function of Space Time

of a naphtha to less than 2 ppm total sulfur at normal reactor conditions.

2. The decrease in the rate of desulfurization could be the result of product inhibition (decrease in the value of A). Hydrogen sulfide has been sighted as a likely villian (5). However, such an inhibiting effect should be a continuous function of the inhibitor's concentration, which would be expected to be a continuous function of space time. Therefore, product inhibition of hydrodesulfurization reactions is an unsatisfactory explanation of a discontinuous reduction in the rate of desulfurization.
3. The reduction in the rate of desulfurization as observed in Figure 2 could be attributed to the presence of uniquely unreactive organosulfur species. However, no sufficiently unreactive specie has been found in the naphtha boiling range.

Therefore, the standard method of hydrodesulfurization data reduction seems to be fundamentally inconsistent with the data presented in Figure 2.

A similar phenomenon was encountered in a study of gas oil desulfurization (6). Increasing space time did not produce conversions above 95% total sulfur removal. The break in the rate of hydrodesulfurization shown in Figure 2 occured at 97% total sulfur conversion.

Approach to Study

The goal of this work will be to gain a mechanistic understanding of the causes of the additional difficulties encountered while desulfurizing a cracked rather than virgin naphtha. Figure 2 shows an abrupt, nearly ten-fold, reduction in the assumed first order rate constant. This work will concentrate on the causes of this reduction in the rate of desulfurization.

Data Source

This analysis will be based on both literature and some experimental data made available from a research laboratory. The data are tabulated and a sketch of the experimental apparatus is given in Appendix A.

CHAPTER II

MODEL DEVELOPMENT

To simplify the discussion, the regions of Figure 2 will be defined as follows:

1. The break point is defined as the space time at which the sharp reduction in the rate of hydrodesulfurization occurs.
2. Low conversion region refers to the kinetics of hydrodesulfurization with space time less than the break point.
3. High conversion region refers to the kinetics with space time greater than the break point.

In the following presentation rather detailed and complex reaction systems are developed by a step-by-step addition of individual reactions. This technique is intended to reduce the difficulty in following the overall development.

The data presented in Figure 2 suggest the possibility that at high conversion of total sulfur, some specie in the reactor could be limiting the net rate of desulfurization. The conversion of thiols and olefins are about equal over the high conversion region (80% and 70% respectively). This suggests a connection between the kinetics of olefin saturation and thiol hydrodesulfurization.

Since thiol and olefin kinetics may be related in the high conversion region, the model development will begin by considering reactions involving these species. Decomposition of ethane thiol over molybdenum disulfide catalyst at 575°F and a total pressure of one atmosphere (Reaction 5) has been shown to yield H_2S and ethylene as the major initial products even with .85 mole fraction hydrogen in the feed (2).

$$C_2H_5SH \xrightleftharpoons[k_5^-]{k_5^+} H_2S + C_2H_4 \qquad (5)$$

Ethane Thiol — Hydrogen Sulfide — Ethylene

The subscript on the rate constant corresponds to the reaction identification number in which the constant was first introduced. The superscript specifies whether the foreward (+) or the reverse (-) reaction is being considered. Since H_2S and ethylene were initially favored products, Reaction 5 must have been more rapid than ethane thiol hydrodesulfurization (Reaction 6).

$$C_2H_5SH + H_2 \xrightarrow{k_6} H_2S + C_2H_6 \qquad (6)$$

Ethane Thiol — Hydrogen — Hydrogen Sulfide — Ethane

Otherwise, ethane, not ethylene, would have been the favored product. However, this work gives no clue to the relative magnitude of the rates of Reaction 5 and hydrodesulfurization of sulfide and ring sulfur compounds. Table I (7) indicates that thiols are the most reactive class of organosulfur specie with respect to hydrodesulfurization. Therefore, if Reaction 5 is much more rapid than thiol hydrogenolysis, then it is probably more rapid than hydrogenolysis of the other classes of organosulfur species (ring sulfur and sulfides). Since ethylene was also a kinetically favored product, Reaction 5 must have been much more rapid than ethylene saturation.

TABLE I (7)

RELATIVE REACTIVITIES OF ORGANOSULFUR SPECIES TO HYDRODESULFURIZATION

Most Reactive.	Benzene Thiol
	Ethane Thiol
	Dibenzyl Sulfide
	3-Methyl-1-butane Thiol
	Diallyl Sulfide
	Diisoamyl Sulfide
Least Reactive	Thiophene

The next step in the analysis will be to consider the role of the decomposition and synthesis of thiols in the desulfurization of thiophene, a common organosulfur specie in petroleum stocks. There is general agreement that the following representation of thiophene hydrodesulfurization (Reactions 7 and 8) is reasonable (8), although superficial.

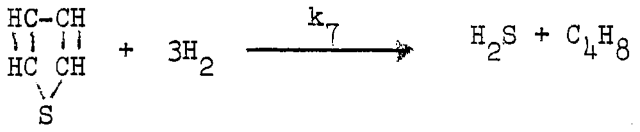

$$\text{Thiophene} + 3H_2 \xrightarrow{k_7} H_2S + C_4H_8 \quad (7)$$

Thiophene Butene

$$C_4H_8 + H_2 \xrightarrow{k_8} C_4H_{10} \quad (8)$$

Butene Butane

The details of the mechanism of catalyzed hydrogenolysis of thiophene in Reaction 7 are beyond the scope of this work. Both Reaction 7 and 8 are essentially irreversible (8). Preliminary runs without catalyst (2) indicate that the rates of non-catalyzed reactions of organosulfur species considered in this work are probably negligible compared to the corresponding catalyzed reaction.

Since a significant amount of butene is usually detected in the bulk gas phase (3, 8), the butene formed on the catalyst surface by Reaction 7 will be assumed to desorb before significant saturation occurs by Reaction 8. Adding the adsorption steps to Reactions 7 and 8 yields Reaction System I and II.

Reaction System I

Partial Thiophene Hydrodesulfurization

$$\underset{(g)}{\text{Thiophene}} \underset{k_9^-}{\overset{k_9^+}{\rightleftarrows}} \underset{(a)}{\text{Thiophene}} \tag{9}$$

$$\underset{(a)}{\text{Thiophene}} + 3H_2 \longrightarrow H_2S + \underset{(g)}{\text{butene}} \tag{7}$$

Reaction System II

Butene Saturation

$$\underset{(g)}{\text{Butene}} \underset{k_{10}^-}{\overset{k_{10}^+}{\rightleftarrows}} \underset{(a)}{\text{Butene}} \tag{10}$$

$$\underset{(a)}{\text{Butene}} + H_2 \xrightarrow{k_8} \text{Butane} \tag{8}$$

A specie adsorbed on the catalyst surface is specified by "(a)" and a non-adsorbed specie in the vicinity of the catalyst surface by "(g)." The disposition of the remaining species between the surface and the gas phase will be specified as needed in the model development.

By analogy, Reaction 5 suggests that butene could readily react with H_2S. Adding this reaction to Reaction System II yields Reaction System III.

Reaction System III

Butene Saturation and
Thiol Production

$$\underset{(g)}{\text{Butene}} \underset{k_{10}^{-}}{\overset{k_{10}^{+}}{\rightleftharpoons}} \underset{(a)}{\text{Butene}} \qquad (10)$$

$$\underset{(a)}{\text{Butene}} + H_2 \xrightarrow{k_8} \text{Butane} \qquad (8)$$

$$\underset{(a)}{\text{Butene}} + H_2S \underset{k_{11}^{-}}{\overset{k_{11}^{+}}{\rightleftharpoons}} \text{Butane Thiol} \qquad (11)$$

Reaction System III suggests that butane thiol should be a product. However, in a study of thiophene desulfurization over a cobalt-molybdate catalyst (3), efforts to detect butane thiol in the bulk gas phase were unsuccessful. In order for Reaction System III to be compatible with this observation, butane thiol must be an adsorbed product and be consumed at the catalyst surface via an additional reaction much more rapidly than it desorbs. In this case, a very low concentration of butane thiol in the bulk gas phase is possible. Probably, some of the butane thiol is consumed by hydrogenolysis (Reaction 12).

$$\underset{(a)}{\text{Butane Thiol}} + H_2 \xrightarrow{k_{12}} H_2S + \text{Butane} \qquad (12)$$

However, Reaction 12 could not alone prevent desorption of butane thiol from the catalyst surface. Earlier arguments indicate that the rate of Reaction 11 should be much more rapid than Reaction 12. Therefore, butane thiol must be consumed at the surface by another reaction.

Reaction 5 suggests that butane thiol is capable of consumption at the surface by decomposition. In order for the decomposition to be effective in preventing desorption of butane thiol, it must occur essentially irreversibly. But, Reaction 5 is reversible. If the products were physically separated upon reaction in a kinetically favored path, then the bulk gas phase concentration of the butane thiol could be held to a very low level. This argument suggests the following path for butane thiol decomposition (Reaction 13).

$$\underset{(a)}{\text{Butane Thiol}} \xrightarrow{k_{13}} \underset{(a)}{H_2S} + \underset{(g)}{\text{Butene}} \qquad (13)$$

Adding Reactions 12 and 13 to Reaction System III yields Reaction System IV.

Reaction System IV

Butene Saturation and Butane
Thiol Production and
Consumption

$$\underset{(g)}{\text{Butene}} \underset{k_{10}^{-}}{\overset{k_{10}^{+}}{\rightleftarrows}} \underset{(a)}{\text{Butene}} \qquad (10)$$

$$\underset{(a)}{\text{Butene}} + H_2 \xrightarrow{k_8} \text{Butane} \qquad (8)$$

$$\underset{(a)}{\text{Butene}} + H_2S \underset{k_{11}^-}{\overset{k_{11}^+}{\rightleftarrows}} \text{Butane thiol} \qquad (11)$$

$$\underset{(a)}{\text{Butane Thiol}} + H_2 \xrightarrow{k_{12}} H_2S + \text{Butane} \qquad (12)$$

$$\underset{(a)}{\text{Butane Thiol}} \xrightarrow{k_{13}} \underset{(a)}{H_2S} + \underset{(g)}{\text{Butene}} \qquad (13)$$

Consider the consequences of H_2S in the vicinity of the catalyst surface (but not adsorbed on the surface) as a reactant in Reaction 11. Earlier, it was argued that Reactions 11 and 13 are more rapid than Reaction 12. If H_2S in the vicinity of the catalyst surface, were the reactant in Reaction 11, then Reactions 11 and 13 would result in the net adsorption of H_2S. However, H_2S has been shown to desorb from a cobalt-molybdate catalyst very slowly (3). If the rate of accumulation of H_2S on the catalyst surface is assumed negligible, then the rate of Reaction 11 and 13 could be no more rapid than the desorption of H_2S from the catalyst surface. Since Reactions 11 and 13 are thought to proceed much more rapidly than H_2S desorption, H_2S should be an adsorbed reactant in Reaction 11.

Notice that the reactants and net products of Reactions 10, 11, and 13 are identical (adsorbed H_2S and butene in the vicinity of the catalyst surface). Reaction System V is a simplified presentation of Reaction System IV.

Reaction System V

Butene Saturation on a Sulfided Catalyst

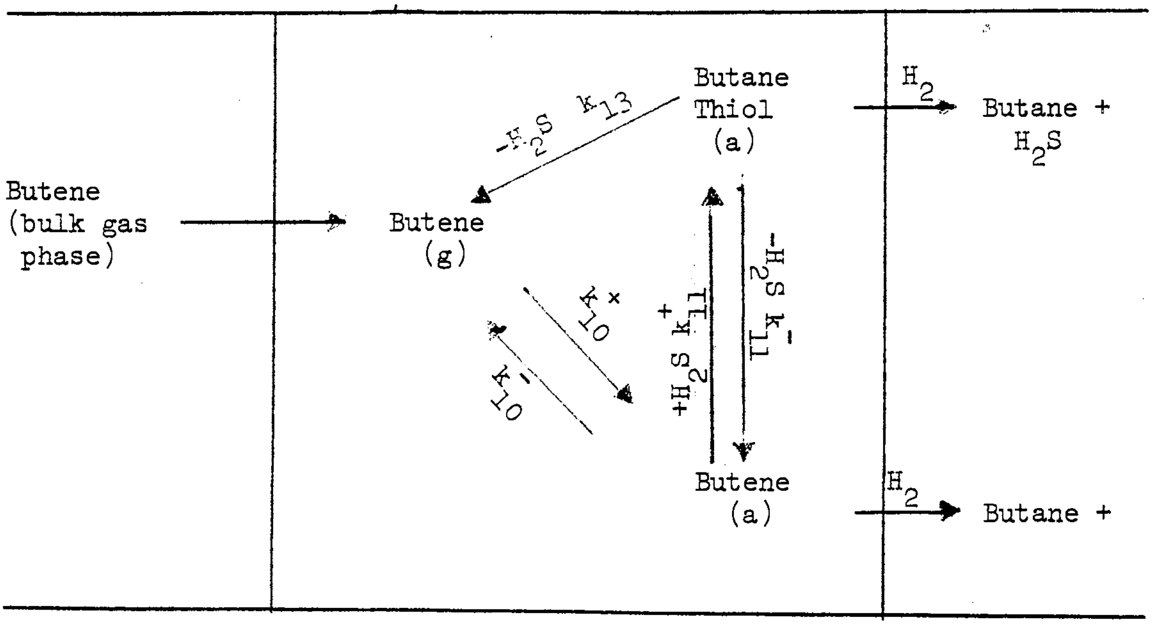

Since petroleum fractions are the typical feed to a commercial HDS reactor, a generalized model is more important (at least from an engineering viewpoint) than a model specifically tailored for a thiophenic feed. Often, the composition of a reformer feed is characterized in terms of classes of hydrocarbon compounds (olefins, aromatics, and paraffins), organic sulfur, and organic nitrogen. Any general model for petroleum hydrodesulfurization, at the present time, must be based on these rather general feed characteristics. With

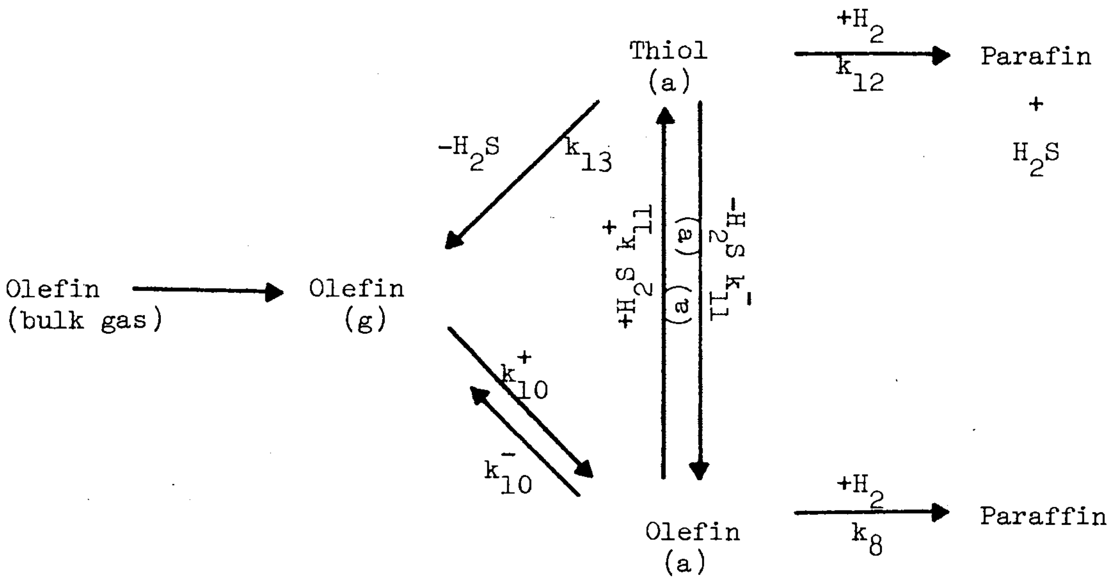

Net Reaction: Olefin + H_2 $\longrightarrow$ Paraffin

Figure 3. Olefin Saturation on a Sulfided Catalyst

the details of Reaction System V as a guide, a scheme in terms of generalized and specific components is shown in Figure 3.

The system of reactions in Figure 3 is a mechanistic representation of the coupling of the kinetics of olefin saturation and hydrodesulfurization. This model was developed primarily from previous pure component studies. However, this system of reactions uses generalized component designation for application to petroleum fraction hydrodesulfurization. In the next chapter, the reactions in Figure 3 will be used to gain a mechanistic understanding of the abrupt reduction in the rate of hydrodesulfurization shown in Figure 2.

CHAPTER III

MODEL TEST

The model test will begin by explicitly defining the model in terms of ten assumptions. Then, it will be used to predict a relationship between olefin and thiol bulk gas phase concentrations and a rate expression for olefin saturation in the high conversion region. Both of the predictions will be tested with the data in Appendix A. Finally, the model will be used to rationalize the sharp reduction in the rate of hydrodesulfurization shown in Figure 2.

The model is defined by the following list of postulates (referenced in the subsequent development as Assumption 1 through Assumption 10).

1. The reactions in Figure 3 are a reasonable representation of olefin saturation on a sulfided cobalt-molybdate catalyst.
2. The net rate of Reaction 11 can be taken as essentially equal to the rate of Reaction 13.
3. Surface concentration of unoccupied active sites on the catalyst surface is nearly constant in the high conversion region.
4. Diffusion resistances between the bulk gas phase and the catalyst surface are negligible. Since mass transfer resistances have been shown to be significant in many heterogeneous reactions, the role of diffusion in

hydrodesulfurization of a cracked naphtha is discussed in Appendix B.

5. Essentially all of the thiols present in the high conversion region were produced by Reaction 11.
6. The rate of accumulation of adsorbed species is negligible (steady state assumption).
7. The rates of all reactions presented in Figure 3 are proportional to the concentration of adsorbed H_2S, olefin, and thiol reactants of the reaction under consideration. Since hydrogen is in excess, the rate of reactions in Figure 3 are assumed to be independent of the relatively small change in its concentration across the reactor.
8. The bromine number (9) of the naphtha is proportional to the olefin concentration. Bromine number is a commonly used measure of unsaturation of a petroleum fractions.
9. Reactants form an ideal gas.
10. Molar flow rates of naphtha and hydrogen are nearly constant in the high conversion region.

The development of a relationship between olefin and thiol bulk gas phase concentrations in the high conversion region will begin by expressing Assumption 2 in terms of the following equality (Equation 14).

$$\begin{matrix}\text{Net Rate of} & & \text{Rate of} \\ \text{Thiol Synthesis} & = & \text{Thiol Consumption} \\ \text{by Reaction 11} & & \text{by Reaction 13}\end{matrix} \qquad (14)$$

Substitutions of the appropriate rate expressions from Assumption 7 into Equation 14 yields Equation 15.

$$k_{11}^{+}C_{O}C_{H_2S} - k_{11}^{-}C_{T} = k_{13}C_{T} \tag{15}$$

Where, C_O, C_{H_2S}, and C_T are the adsorbed olefin, hydrogen sulfide, and thiol concentrations. A rearrangement of Equation 15 yields Equation 16.

$$\frac{C_T}{C_O} = \frac{k_{11}^{+}\ C_{H_2S}}{k_{11}^{-} + k_{13}} = k_{16} \tag{16}$$

C_{H_2S} in Equation 16 will be evaluated using a material balance (Equation 17) of adsorbed hydrogen sulfide.

$$\begin{array}{c}\text{Rate of } H_2S\\ \text{Adsorption}\end{array} = \begin{array}{c}\text{Rate of } H_2S\\ \text{Desorption}\end{array} + \begin{array}{c}\text{Rate of } H_2S\\ \text{Accumulation}\\ \text{on Catalyst}\end{array} + \begin{array}{c}\text{Rate of } H_2S\\ \text{Consumption}\\ \text{on Catalyst}\end{array} \tag{17}$$

Assumptions 2, 4, and 6 suggest that, in the high conversion region, Equation 17 is essentially equivalent to Equation 18.

$$\begin{array}{c}\text{Rate of } H_2S\\ \text{Adsorption}\end{array} = \begin{array}{c}\text{Rate of } H_2S\\ \text{Desorption}\end{array} \tag{18}$$

Substitution of the appropriate rate expressions into Equation 18 yields Equation 19.

$$k_{19}^{+}\ C_E\ P_{H_2S} = k_{19}^{-}\ C_{H_2S} \tag{19}$$

C_E is the concentration of unoccupied active sites and P_{H_2S} is the partial pressure of H_2S in the bulk gas phase. Rearranging Equation 19 gives Equation 20.

$$C_{H_2S} = \frac{k_{19}^{+} C_E}{k_{19}^{-}} P_{H_2S} = k_{20} \tag{20}$$

Assumption 3 asserts that C_E is a constant in the high conversion region. The data in Appendix A show that P_{H_2S} is essentially constant over the high conversion region. Therefore, Equation 20 predicts that C_{H_2S} is essentially a constant in the high conversion region. Substitution of this result into Equation 16 shows that thiol and olefin catalyst surface concentrations should be related by a simple proportionality. Since it is difficult, if not impossible, to monitor the concentrations of adsorbed species, the surface concentrations must be related to the bulk gas phase concentrations before this hypothesis can be tested.

A material balance (Equation 21) of adsorbed thiols will be used to relate the bulk gas phase and catalyst surface thiol concentrations.

$$\begin{array}{l}\text{Rate of}\\ \text{Thiol}\\ \text{Adsorption}\end{array} = \begin{array}{l}\text{Rate of}\\ \text{Thiol}\\ \text{Desorption}\end{array} + \begin{array}{l}\text{Rate of}\\ \text{Thiol}\\ \text{Accumulation}\\ \text{on Catalyst}\end{array} + \begin{array}{l}\text{Rate of}\\ \text{Thiol}\\ \text{Consumption}\\ \text{on Catalyst}\end{array} \tag{21}$$

Assumption 6 makes Equation 21 equivalent to Equation 22.

$$\begin{array}{l}\text{Rate of}\\ \text{Thiol}\\ \text{Adsorption}\end{array} = \begin{array}{l}\text{Rate of}\\ \text{Thiol}\\ \text{Desorption}\end{array} + \begin{array}{l}\text{Rate of Thiol}\\ \text{Consumption}\\ \text{on the catalyst}\end{array} \tag{22}$$

Substituting standard rate expression forms for reactions presented in Figure 3 into Equation 22 yields Equation 23.

$$k^{+}_{23}\, C_E\, P_T = k^{-}_{23}\, C_T + k^{-}_{11}\, C_T + k_{13}\, C_T + k_{12}\, C_T - k^{+}_{11}\, C_{H_2S}\, C_0 \tag{23}$$

P_T is the thiol partial pressure in the bulk gas phase. Combining Equations 16, 20, and 23 yields Equation 24.

$$\frac{P_T}{C_T} = \frac{k^{-}_{23} + k^{-}_{11}\, k_{12} + k_{13} - k^{+}_{11}\, k_{20}/k_{16}}{k^{-}_{23} C_E} = \frac{k_{24}}{C_E} \tag{24}$$

Since C_E is assumed to be essentially constant in this region, Equation 24 predicts that the bulk gas phase thiol partial pressure is proportional to the catalyst surface thiol concentration.

The relationship between adsorbed and gas phase olefin concentrations will also be determined by material balance (Equation 25).

$$\begin{array}{l}\text{Rate of}\\ \text{Olefin}\\ \text{Adsorption}\end{array} = \begin{array}{l}\text{Rate of}\\ \text{Olefin}\\ \text{Desorption}\end{array} + \begin{array}{l}\text{Rate of Olefin}\\ \text{Accumulation}\\ \text{on the Catalyst}\end{array} + \begin{array}{l}\text{Rate of Olefin}\\ \text{Consumption}\\ \text{on the Catalyst}\end{array} \tag{25}$$

Assumption 6 makes Equation 25 equivalent to Equation 26.

$$\begin{array}{l}\text{Rate of}\\ \text{Olefin}\\ \text{Adsorption}\end{array} = \begin{array}{l}\text{Rate of}\\ \text{Olefin}\\ \text{Desorption}\end{array} + \begin{array}{l}\text{Rate of Olefin}\\ \text{Consumption}\\ \text{on the Catalyst}\end{array} \tag{26}$$

Substitution of the appropriate rate expression into Equation 26 gives Equation 27.

$$k^{+}_{10}\, P_0\, C_E = k^{-}_{10}\, C_0 + k_8\, C_0 + k^{+}_{11}\, C_0\, C_{H_2S} - k^{-}_{11}\, C_T \tag{27}$$

Where, P_0 is the partial pressure of olefins in the bulk gas phase. Combining Equations 16, 20, and 27 yields Equation 28.

$$\frac{P_O}{C_O} = \frac{k_{10}^{-} + k_8 + k_{11}^{+} k_{20} - k_{11}^{-} k_{16}}{k_{10}^{+} C_E} = \frac{k_{28}}{C_E} \qquad (28)$$

The bulk gas phase olefin and thiol partial pressures can be related by combining Equations 16, 24, and 28 to give Equation 29.

$$P_O = \left(\frac{k_{28}}{k_{16}\, k_{24}}\right) P_T = k_{29}\, P_T \qquad (29)$$

Assumption 9 makes Equation 29 equivalent to Equation 30.

$$y_O = k_{30} y_T \qquad (30)$$

Where, y_O and y_T are the olefin and thiol mole fractions in the bulk gas phase. Since the molar flow rates of hydrogen and naphtha are thought to be nearly constant over the high conversion region (Assumption 10), Equation 31 is equivalent to Equation 30.

$$Br = k_{31}\, S_T \qquad (31)$$

Where, Br and S_T are the bromine number (previously assumed to be proportional to the olefin concentration in the naphtha) and thiol concentration in the oil, ppm. Equation 31 predicts that, in the high conversion region, a plot of the thiol concentration as a function of bromine number should yield a straight line with intercept at the origin. Figure 4 shows that this prediction is supported by the data in Appendix A. Data from Appendix A are presented for experiments with one reactor (1RX) and two reactors in series (2RX) at constant temperature, pressure, and space time. However, the superficial gas

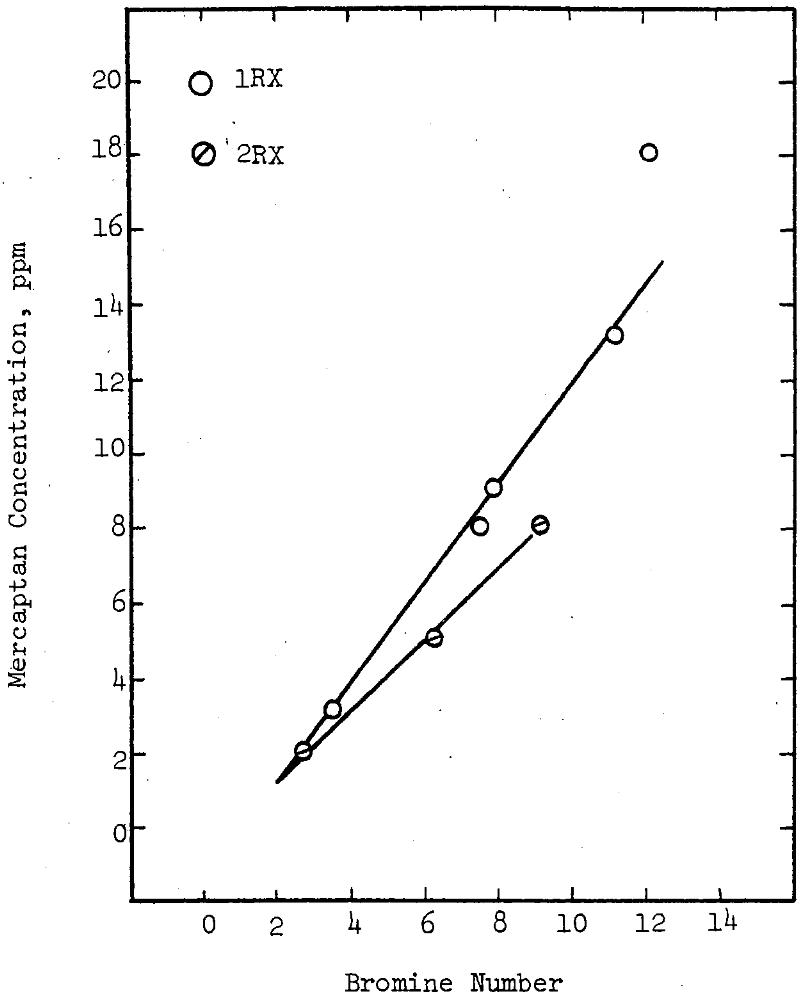

Figure 4. Mercaptan Concentration as a Function of Bromine Number in the High Conversion Region

velocity in the two reactor runs is double the velocity of the corresponding single reactor runs.

Development of a rate expression for olefin saturation in the high conversion region will begin by writing an expression, Equation 32, for the overall rate of olefin saturation.

$$\begin{array}{l}\text{Rate of}\\\text{Olefin}\\\text{Saturation}\end{array} = \begin{array}{l}\text{Rate of}\\\text{Reaction 8}\end{array} + \begin{array}{l}\text{Rate of}\\\text{Reaction 12}\end{array} \tag{32}$$

Substituting the appropriate rate expressions into Equation 32 gives Equation 33.

$$\begin{array}{l}\text{Rate of}\\\text{Olefin}\\\text{Saturation}\end{array} = k_8\ C_O + k_{12}\ C_T \tag{33}$$

Combining Equations 16, 28, and 33 yields Equation 34.

$$\begin{array}{l}\text{Rate of}\\\text{Olefin}\\\text{Saturation}\end{array} = \left(\frac{k_8 + k_{12}\ k_{16}}{k_{28}}\right) P_O\ C_E \tag{34}$$

Assumptions 3, 9, and 10 make Equation 34 equivalent to Equation 35.

$$\begin{array}{l}\text{Rate of}\\\text{Olefin}\\\text{Saturation}\end{array} = - \frac{dBr}{d\Theta} = k_{35}\ Br \tag{35}$$

Integration of Equation 35 gives Equation 36.

$$\ln Br^{\Theta} = - k_{36}\ \Theta + \ln Br^{o} \tag{36}$$

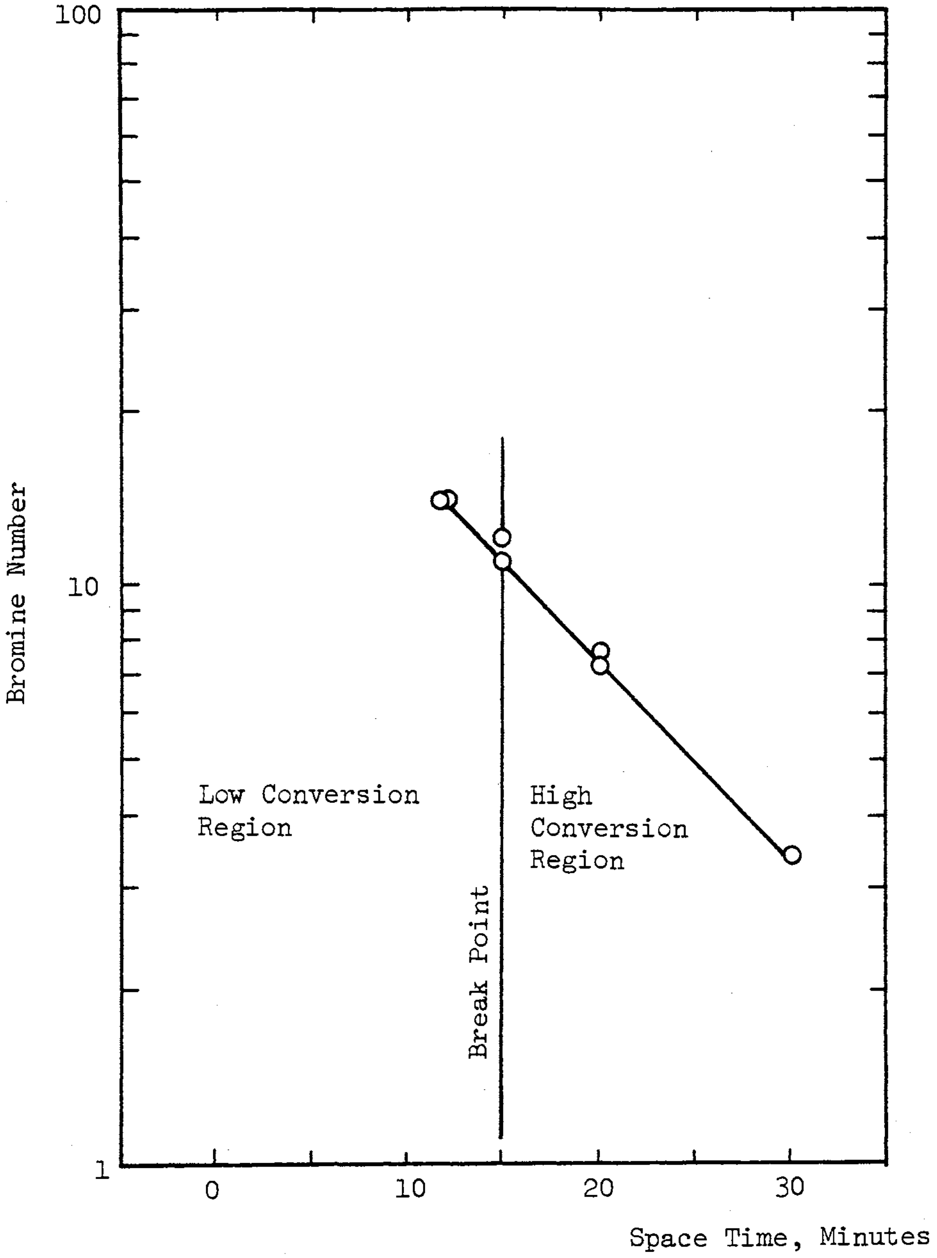

Figure 5. Olefin Saturation Kinetics in the High Conversion Region

Where, Br^{o} and Br^{θ} are the initial and outlet bromine number with space time θ. Therefore, a plot of the logarithm of bromine number as a function of space time should yield a straight line. Figure 5 shows that the data in Appendix A support this prediction in the high conversion region.

Verification of the forms of Equation 31 and 36 with the data in Appendix A suggest that the model is a reasonable qualitative representation of hydrodesulfurization of a cracked naphtha. The next step will be to use the model to speculate on the causes for the abrupt reduction in the rate of hydrodesulfurization shown in Figure 2.

Figure 3 postulates that thiols are an intermediate product of olefin saturation on a sulfided cobalt-molybdate catalyst. A previous work (2) has shown that thiols are capable of adding to olefins to form sulfides on a molybdenum disulfide catalyst. The break point is thought to be the space time at which the thiol and sulfide synthesis rate approaches the rate of desulfurization. Therefore, the sharp reduction in the rate of desulfurization shown in Figure 2 is the result of these competing organosulfur synthetic reactions.

CHAPTER IV

HDS REACTOR SIZING PROCEDURE

In order for the model developed in previous chapters to be useful, from a practical engineering viewpoint, it must be applied to commerical processes. The model will be used as a basis for a procedure to size a commerical HDS reactor to pretreat a reformer feed.

Since data for only one feed and one set of operating conditions were analyzed, it is impossible to suggest a procedure to a priori predict the reactor size required to achieve a specified organosulfur conversion. This work will present a method to size a HDS reactor using pilot plant data at the design operating condition. Hopefully, as the body of hydrodesulfurization data of a cracked naphtha feed becomes more complete, a generalized reactor sizing procedure could be developed using principles presented here.

Economic reformer operation requires a hydrodesulfurizer outlet total sulfur concentration in the vicinity of one ppm (1). Therefore, the procedure need only to be capable of predicting the reactor size required to obtain this outlet concentration.

The model asserts that the rate of hydrodesulfurization and organosulfur synthetic reactions are nearly equal in the high conversion region. The observed net desulfurization is thought to result from the saturation of olefins, a common reactant for all postulated organosulfur synthetic reactions. This analysis suggests that either the rate of hydrodesulfurization or olefin saturation could set the size of reactor required to obtain a one ppm total sulfur outlet concentration. The following three step procedure is proposed:

1. Calculate the size of HDS reactor required to hydrodesulfurize to one ppm total sulfur assuming the rate of desulfurization is controlling.
2. Calculate the reactor size required to obtain one ppm total sulfur assuming that the rate of olefin saturation is controlling.
3. Size the reactor based on the space time calculated in Steps 1 and 2 that is larger.

If the rate of hydrodesulfurization were controlling, then the required space time could be calculated by evaluating the appropriate desulfurization rate expression. Figure 2 shows that at low conversion of total sulfur, a plot of the logarithm of sulfur concentration as a function of space time yields a straight line. This indicates that the space time required to hydrodesulfurize to one ppm total sulfur assuming desulfurization reactions controlled may be calculated by Equation 37.

$$\Theta = \frac{\log_{10} S^{o}_{TS}}{k_{37}} \tag{37}$$

S^{o}_{TS} is the reactor feed total sulfur concentration, ppm, and k_{37} is the slope of a plot of the common logarithm of total sulfur concentration, ppm, as a function of space time in the low conversion region of pilot plant data at the proposed design operating conditions.

The required space time to desulfurize to one ppm total sulfur assuming that the rate of olefin saturation controls will be calculated using the following two step procedure:

1. Determine the bromine number as a function of space time using pilot plant data at the proposed operating conditions. The model predicts that olefin saturation is first order with respect to olefin concentration. An earlier work (3) has concluded that H_2S is a reversible poison for olefin saturation. Therefore a Hougen and Watson (11) rate expression, Equation 38, might be expected to describe olefin saturation kinetics.

   $$\begin{matrix}\text{Rate of}\\ \text{Olefin}\\ \text{Saturation}\end{matrix} = \frac{dBr}{d\Theta} = \frac{-k_{38}Br}{bX + 1} \qquad (38)$$

   X is the fraction of organosulfur species in the reactor feed that has been hydrodesulfurized at any space time Θ. Integration of Equation 38 yields Equation 39.

   $$\log_{10}\left(\frac{Br^{o}}{Br^{\Theta}}\right) = \int_0^{\Theta} \frac{k_{39}\ d\Theta}{bX + 1.} \qquad (39)$$

   Br^{o} and Br^{Θ} are the initial and outlet bromine number of a reactor with space time Θ. A simplified procedure for estimating k_{39} and b is given in the numerical example in Appendix C.

2. Determine the required outlet bromine number to desulfurize to the region of one ppm total sulfur. Extrapolation of the of the relation presented on Figure 4 indicates that, for the

feed used in this work, a bromine number in the region of .9 is required to obtain a negligible sulfur level. However, more data are needed to determine the required outlet bromine number as a function of H_2S partial pressure and reactor operating conditions.

The sizing procedure is completed by selecting the larger space time to size the reactor. A numerical example using the data in Appendix A is given in Appendix C.

CHAPTER V

CONCLUSIONS AND RECOMMENDATION

Conclusions

The original goal of this work was to suggest a mechanistic rationalization for the observation that a cracked naphtha is more difficult to hydrodesulfurize than a virgin naphtha. Analysis showed that at very high conversions of total sulfur, reactions involving the addition of H_2S and thiols to olefins can drastically reduce the net rate of desulfurization. Since the olefin content of a cracked naphtha is typically much greater than a virgin naphtha, the additional difficulties encountered while desulfurizing a cracked rather than a virgin stock are probably due to organosulfur synthetic reactions.

A tentative design procedure was proposed to account for the effect of olefins in an HDS reactor. However, additional pilot plant and refinery data are needed to test the viability of this design procedure.

Probably the most important result of this work is the observation that both desulfurization and olefin saturation activity must be considered when optimizing the activity of a HDS catalyst to hydrodesulfurize a cracked naphtha to one ppm total sulfur.

Recommendation

The logical extension of this work would be to test usefulness of the design procedure using refinery operating data. Particular attention should be directed toward testing the validity of the olefin saturation criteria for hydrodesulfurization of a cracked naphtha to one ppm total sulfur.

SELECTED BIBLIOGRAPHY

(1) Schuman, S. C., and Shalt, H., Catalysis Reviews, 4(2), p. 287 (1970).

(2) Kieran, P., and Kembal, C., Journal of Catalysis, 4, p.p. 380-393 (1965).

(3) Owens, P. J., and Amberg, C. H., Advances in Chemistry Series, 33, p.p. 182-197.

(4) McKinley, P. J., in Catalysis (P. H. Emmett, ed), Vol. V, p.p. 421-422.

(5) Metcalfe, T. B., paper presented at Hydrodesulfurization Symposium, 64th National A.I.Ch.E. meeting, New Orleans, La., March 18, 1969.

(6) Schuman, S. C., and Shalt, H., Catalysis Reviews, 4(2) p. 271 (1970).

(7) Schuman, S. C., and Shalt, H., Catalysis Reviews, 4(2), p. 270 (1970).

(8) Satterfield, C. N., and Roberts, G. W., A.I.Ch.E. Journal, 14 (1), p. 159 (1968).

(9) _____, 1971 Annual Book of ASTM Standards, Part 18, standard designation D 1159.

(10) Satterfield, C. N., Mass Transfer in Heterogeneous Catalysis, M.I.T. Press, Cambridge, Mass. (1970), p.p. 79-86.

(11) Hougan, O. A., and Watson, K. M., Industrial Engineering Chemistry, 35(5), p. 529, 1943.

APPENDIX A

DATA

Table II presents olefin, thiol, and total sulfur removal as a function of space time at constant temperature ($600^{o}F$), pressure (300 psig) and hydrogen flow rate (800 SCF/bbl) for a cracked naphtha feed in a pack bed reactor. Figure 6 is a sketch of the experimental apparatus.

TABLE II

DESULFURIZATION DATA

CONSTANT OPERATING CONDITIONS

Temperature	600 °F
Pressure	300 psig
Hydrogen Rate	800 SCF/bbl
Feed Bromine Number	44.0
Feed Total Sulfur	780.

RUN NUMBER	1	2	3	4	5	6	7	8	9	10	11	12
VARIABLE OPERATING CONDITIONS												
Oil Feed Rate, ml/hr	720	1090	1440	1810	360	540	720	910	360	540	720	900
Number of Reactors in Series	2	2	2	2	1	1	1	1	1	1	1	1
Hydrogen Rate, SCFH*	3.6	5.4	7.2	9.1	1.82	2.7	3.6	4.5	1.82	2.7	3.6	4.5
Space Time, minutes	30	20	15	12	30	20	15	11.8	30	20	15	12
PRODUCT ANALYSIS												
Total Sulfur, ppm	19	17	30	47	14	21	22	45	16	19	20	46
Mercaptan Sulfur, ppm	2	5	8	7	3	9	13	15	3	8	18	17
Bromine Number	2.7	6.2	9.0	12	3.5	7.7	11	14	3.5	7.3	12	14

---

* Standard Cubic Feet per Hour

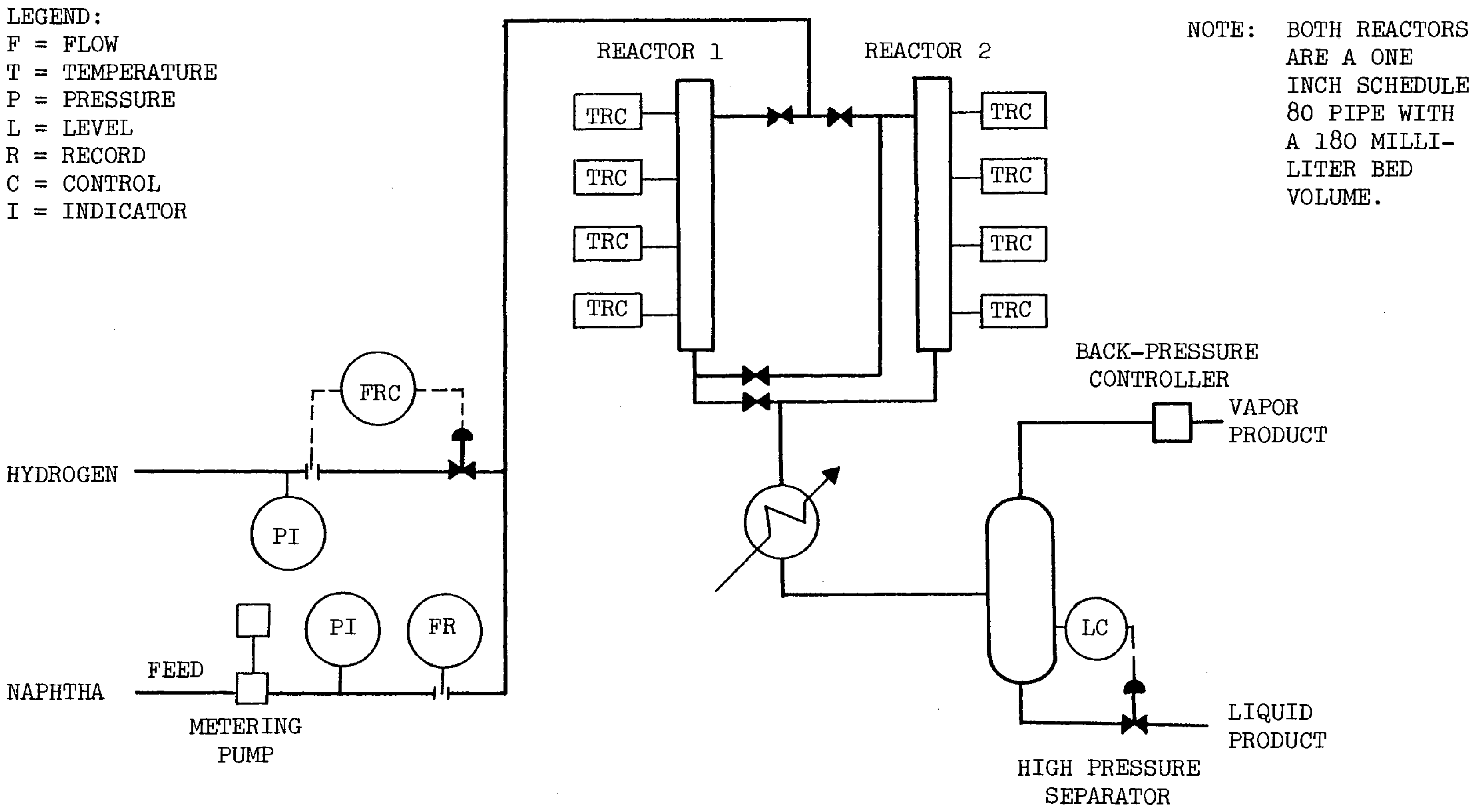

Figure 6. Experimental Apparatus

APPENDIX B

DIFFUSION EFFECTS

Theoretically, the effect of film diffusion resistance between the main gas stream and the catalyst pellet can be estimated by doubling the superficial gas velocity while holding temperature, pressure, and space time constant. Figures 7 and 8 present the results of this type of experiment for hydrotreating olefins and organosulfur species in a cracked naphtha. The complete film diffusion control line assumes that the film diffusion coefficient is proportional to the superficial gas velocity to the .641 power (10). These data suggest that film diffusion is a significant resistance to olefin saturation but a negligible resistance to hydrodesulfurization. This is a surprising result since the pseudo-first-order-rate-constant for hydrodesulfurization (slope of curve on Figure 2) is greater than that for olefin saturation (slope of curve on Figure 9). If the diffusivities of all classes of compounds in the naphtha were identical and simple first order kinetics prevailed, then one would expect that the diffusion effect would be most significant in case of the reaction with the higher first order rate constant. However, Figure 8 suggests this is not the case. A theoretical estimate of the maximum mass transfer rate between the bulk gas stream and the catalyst surface will be made to clarify the role of diffusion in hydrotreating a cracked naphtha.

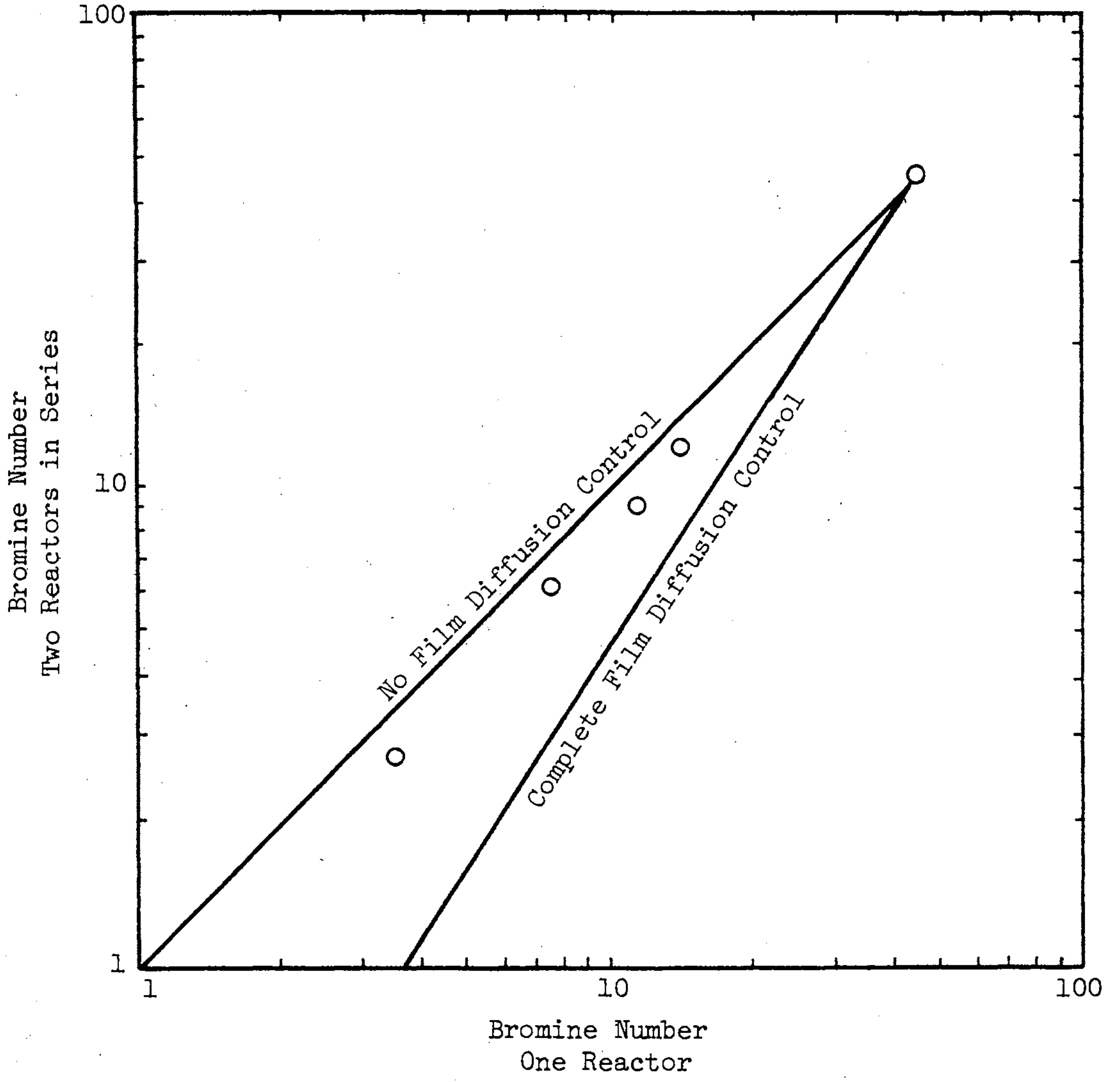

Figure 7. Effect of Film Diffusion in Hydrotreating Olefins of a Cracked Naphtha

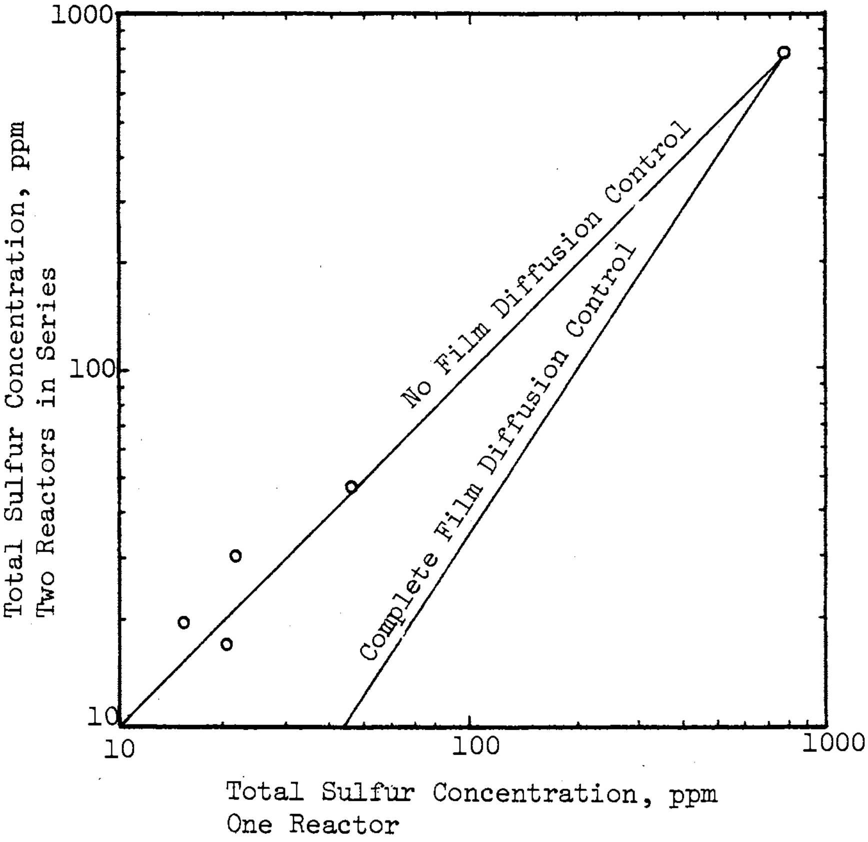

Figure 8. Effect of Film Diffusion in Desulfurization of a Cracked Naphtha

If film diffusion between the bulk gas stream and the catalyst pellet outer surface were controlling the rate of reaction, then the conversion may be estimated using Equation 40 (10).

$$\ln\left(\frac{y_i^o}{y_i^f}\right) = \frac{3.2_z}{dp\ N_{RE}^{.359}\ N_{SC}^{2/3}} \tag{40}$$

Where, y^o and y^f are the reactant bulk gas phase concentration at the reactor inlet and outlet; z and dp are the catalyst bed height and diameter of a sphere with the same surface area as the catalyst pellet. N_{RE} and N_{SC} are the Reynolds and Schmidt numbers. Evaluating Equation 40 for the reactor conditions studies gives Equation 41.

$$\ln\left(\frac{y^o}{y^f}\right) = \frac{(3.2)(38\text{cm})}{(.329\text{cm})(300)^{.359}(2.9)^{2/3}} = 23. \tag{41}$$

This conversion is many orders of magnitude greater than the experimentally observed conversion. This suggests that film diffusion has a negligible effect on olefin saturation and hydrodesulfurization. Theoretical calculations also indicate the effectiveness factor (ratio of actual rate for the whole pellet to the rate evaluated at the outer surface conditions) is nearly one. Although considerable doubt concerning the role of diffusion in hydrotreating a cracked naphtha remains, developments in previous chapters assumed that diffusion resistances are negligible.

APPENDIX C

SAMPLE DESIGN CALCULATIONS

The following calculations are based on the design procedure outlined in Chapter IV and data presented in Appendix A.

Step 1.

A. Calculate k_{37}.

By definition, k_{37} is the slope of a plot of the common logarithm of sulfur concentration, ppm, as a function of space time. A linear regression of the data presented in Appendix A for one reactor yields a value of .105 minutes^{-1} for k_{37}.

B. Calculate the required space time (hydrodesulfurization controlling).

The required space time to desulfurize to 1 ppm total sulfur, assuming that this conversion can be obtained in the low conversion region, is calculated in Equation 42 by evaluating Equation 37.

$$\theta = \frac{\log_{10} S^{o}_{TS}}{k_{37}} = \frac{\log_{10} (780)}{.105} = 28 \text{ Minutes} \qquad (42)$$

Step 2.

A. Determine k_{39} and b.

Equation 43 gives an approximate relationship between k_{39} and b.

$$k_{39} = S_{HC} (b X_{HC} + 1.) \tag{43}$$

Where, S_{HC} is the slope of a plot of the common logarithm of the bromine number as a function of space time in the high conversion region. X_{HC} is the average fractional conversion of organosulfur species in the high conversion region. X_{HC} and S_{HC} have the values of .98 and .034 respectively for the single reactor runs. Then the values of k_{39} can be determined by a trial and error integration of Equation 39. Calculations yield values of .06 minutes^{-1} and .77 for k_{39} and b. Figure 9 shows that Equation 39 is a reasonable rate expression for olefin saturation.

B. Calculate required space time (olefin saturation controlling). Integration of Equation 39 using the above values for k_{39} and b shows that a space time of 48 minutes would be required to obtain a bromine number of .9.

Step 3.

Since the required space time of 48 minutes calculated in Step 2 is greater than 28 minutes of Step 1, a space time of approximately 48 minutes would be needed to obtain one ppm total sulfur in the product at the reactor operating conditions studied.

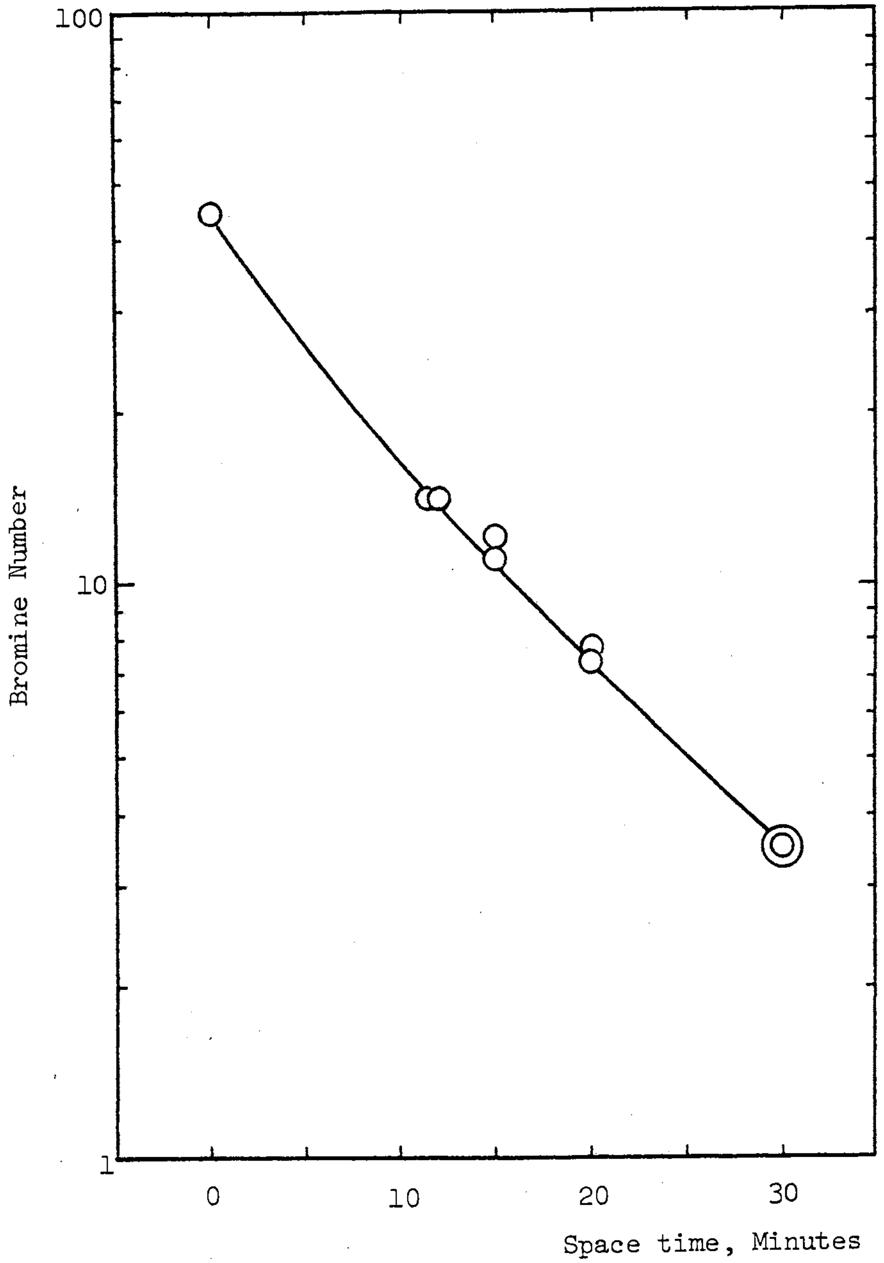

Figure 9. Comparison of Final Form of Olefin Saturation Rate Expression with Data

Replaced
5-10-06

VITA

Donald Prentice Satchell, Jr.

Candidate for the Degree of

Master of Science

Thesis: EFFECT OF OLEFINS ON HYDRODESULFURIZATION OF A CRACKED NAPHTHA REFORMER FEED

Major Field: Chemical Engineering

Biographical:

Personal Data: Born in Lansing, Michigan, April 18, 1947, to Donald and Clara Satchell.

Education: Attended elementary school at State College, Pennsylvania; graduated in 1965 from Westfield High School, Westfield, New Jersey; received the degree of Bachelor of Science in Chemical Engineering at Michigan State University, East Lansing, Michigan on June 22, 1969. Completed requirements for the Master of Science Degree in Chemical Engineering at Oklahoma State University in July, 1972.